[5]S. T. Picraux and F. L. Vook, Phys. Rev. B 18, 2066 (1978); S. T. Picraux, F. L. Vook, and H. J. Stein, in Proceedings of the International Conference on Defects and Radiation Effects in Semiconductors, Nice, France, September 1978 (to be published).

[6]H. J. Stein and P. S. Peercy, Appl. Phys. Lett. 34, 604 (1979).

[7]Presented in brief by H. J. Stein, Bull. Am. Phys. Soc. 24, 435 (1979).

[8]G. D. Watkins, J. Phys. Soc. Jpn. 18, 22 (1963), and *Radiation Damage in Semiconductors* (Academic, New York, 1965), p. 97.

[9]H. J. Stein, in *Radiation Effects in Semiconductors*, edited by J. W. Corbett and G. D. Watkins (Gordon and Breach, New York, 1979), p. 125.

[10]K. L. Brower, in *Ion Implantation in Semiconductors*, edited by F. Chernow, J. A. Borders, and D. K. Brice (Plenum, New York, 1976), p. 427.

Observation of Singular Behavior in the Focusing of Ballistic Phonons in Ge

J. C. Hensel and R. C. Dynes
Bell Laboratories, Murray Hill, New Jersey 07974
(Received 3 August 1979)

High-resolution heat-pulse experiments reveal that transverse, ballistic phonons in Ge are focused into sharply defined beams along the [001] and [110] axes. Angular distributions within these beams display fine-structure representing focusing singularities. It is shown that these features are dependent in a sensitive way on the topology of the phonon-frequency surface.

In pure crystalline dielectric solids at low temperatures the propagation of high-frequency acoustic phonons is ballistic in nature.[1] Elastic anisotropy of the solid imparts directional characteristics to the bassistic propagation—an effect called "phonon focusing."[2,3] In a heat-pulse experiment in Ge distinguished by high angular resolution and wide angular coverage we have discovered a number of remarkable features in the focusing patterns quite unlike anything reported heretofore, *viz*: (1) the transverse acoustical (TA) phonons preferentially radiate in very strong, but narrow (a few degrees width) and sharply defined beams centered on the crystallographic axes [001] and [110]; (2) within these focusing "cones" there appear even sharper spikes representing focusing singularities. In this Letter we show that these observations lead to new insights into the physics of phonon propagation. Besides their obvious relevance to phonon optics,[4] high-frequency phonon generation and propagation, Kapitza resistance,[1] and low-temperature thermal conductivity,[5] these developments are particularly timely since it appears that the strong directionality of phonon focusing is partly responsible (via the phonon wind mechanism[6,7]) for the highly anisotropic shape of the electron-hole droplet cloud, a matter currently being investigated intensively.

Basically, phonon focusing, the concentration of phonon flux along certain directions, depends upon the fact that in anisotropic medium the direction of energy propagation, given by the group velocity vector $\vec{v}_g$, does not necessarily coincide with the phase velocity $\vec{v}_p$, a vector parallel to the phonon wave vector $\vec{k}$. Since the direction of $\vec{v}_g$ is given by the normal to the constant-frequency surface (ω surface), focusing will arise when, as a result of elastic anisotropy, the surface departs from a spherical shape—an extreme but simple example being a cube for which phonon intensity is finite only for directions parallel to the cubic axes and zero otherwise. Obviously focusing effects will be quite sensitive to details of the ω surface as we shall demonstrate.

The experiments were performed in liquid He II at ~ 1.8 K and can be visualized from the inset in Fig. 1. The sample, in the shape of a hemicylinder, can be rotated about its axis by means of a shaft connected to a goniometer at the top of the cryostat. Heat pulses are generated optically by a Q-switched yttrium aluminum garnet laser (pulse width 150 nsec) beam focused on the cylindrical surface which is cylindrical surface which is coated with an evaporated Constantan film. Power densities were kept low, ≈ 1 W/mm^2, to avoid formation of a hot spot.[7] The detector is a thin-film granular Al superconducting bolometer in the form of a narrow stripe aligned with the axis of rotation. Its dimensions, 0.1 mm wide by 1.0 mm long, define the overall angular resolution for the experiment: $\pm 2.9°$ in vertical

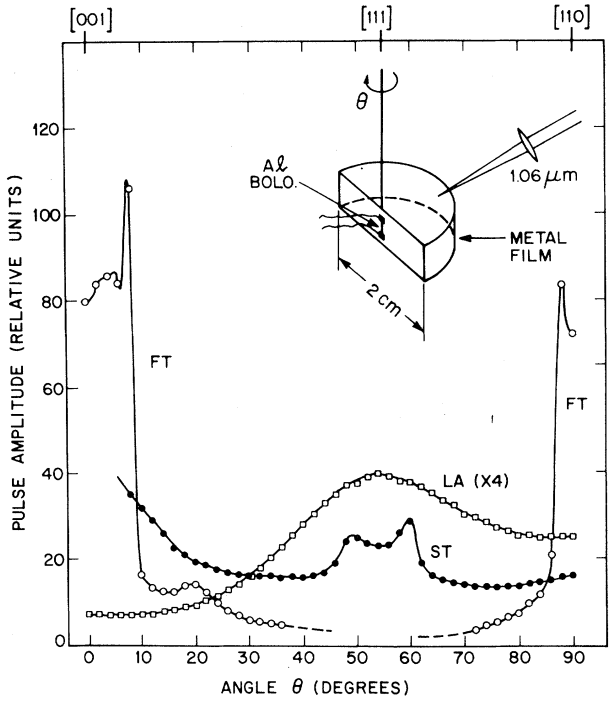

FIG. 1. Angular dependence of phonon focusing in the $(1\bar{1}0)$ plane of Ge (θ is the polar angle referred to the [001] axis). In this scan the boxcar gate position was adjusted at each step to track the phonon peak. Data are corrected for the angular dependence of the flux subtended by the bolometer (Lambert's law). The experimental geometry is shown schematically in the inset.

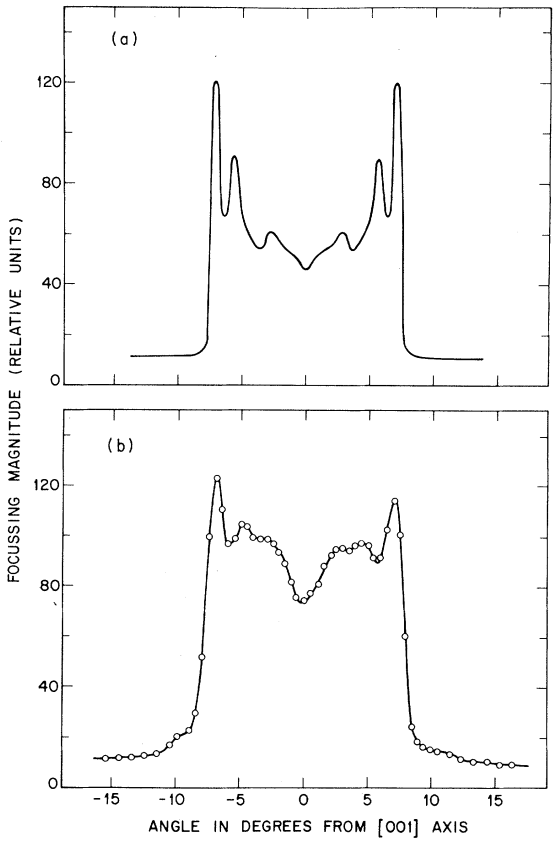

FIG. 2. Fine structure in the focusing of the ST mode (cf. Fig. 1) in the vicinity of the [001] axis [$(1\bar{1}0)$ plane]. Panel (a) shows a calculated angular distribution (see text). Experimental data (circles) are given in panel (b).

plane and ± 0.3° in horizontal plane. The phonon mode spectrum was time resolved with either a boxcar integrator or a Biomation model 8100 transient analyzer.

We plot in Fig. 1 angular distributions in the $(1\bar{1}0)$ plane of the measured pulse heights for the principal acoustic-phonon modes[8]: longitudinal (L), fast transverse (FT), and slow transverse (ST). The L mode varies smoothly from a minimum along [001], a defocusing direction, to a maximum along [111], a focusing direction, in qualitative agreement with Taylor, Maris, and Elbaum.[3] More interesting is the situation for the transverse modes, especially FT. The behavior of this mode is quite extraordinary as one nears the [001] and [110] axes, where it suddenly jumps an order of magnitude in intensity. The transitions occur within a $\Delta\theta$ of less than 1°, peaking at ± 7.0° from (001) and ± 2.0° from [110]. Clearly a very substantial fraction of the total TA-phonon flux is concentrated within these conical regions. A curious feature of the FT angular pattern is the sharp spikes at the cone edges, suggestive of a "resonance" or singularity in the phonon focusing. As we shall see, these are indeed singularities and their width is determined by the experimental angular resolution.

There is nothing distinctive as far as the ST mode is concerned except the appearance of two peaks, one on either side (± 5.5°) of the [111] direction. This structure stems from some topological anomalies in the ω surfaces resulting from the degeneracy of the two transverse modes in this direction (a phenomenon called conical refraction[2]).

The structure for the FT mode in the vicinity of the [001] axis is shown in more detail in Fig. 2. We see that there are actually *two* sets of focusing singularities, one at ± 7° and one at ± 5°. There is in addition a broader shoulder located approximately at ± 3°.

These phenomena can be understood qualitative-

ly from the following simple two-dimensional example. Consider the geometrical constructions in Fig. 3. Figure 3(a) contains a representative phase-velocity "surface," i.e., the locus of $\vec{v}_p$ as a function of $\vec{k}$ [such as one might find in the $(1\bar{1}0)$ plane for Ge]. Derived from (a) in accordance with the mapping $\vec{v}_p = \omega/\vec{k}$ is the "inverse" surface or ω surface shown in (b), and subsequently the group-velocity surface in (c) [$\vec{v}_g = \partial\omega/\partial\vec{k}$ being a vector normal to the ω surface in (b)]. Now the normal vector shown at A in (b) is parallel to k_y and, therefore, maps onto A' in (c); likewise the normal at C is parallel to k_y and maps onto the same axis, but not necessarily at the same magnitude, i.e., at C'. Intermediate points have negative slope and map into the second quadrant, e.g., $B \rightarrow B'$. Point B is, in fact, the point of inflection which gives rise to a cusp at B'. Points from C to D map smoothly from the k_y axis (at C') to the k_x axis (at D'); thereupon a similar structure is generated around the k_x axis. All of the vectors in (b) from A to just beyond C are compressed into a comparatively small region of $\vec{v}_g$ space in (c), the net result being the sharp cone of focusing near [001] which we see in Figs. 1 and 2. Vectors from C to D are mapped into the expanded region C' to D' producing a defocusing. Note in particular that B is an inflection point, i.e., zero curvature, so that an infinity of $\vec{k}$'s maps onto a single point B'. In other words B' is a point of accumulation in the density of states giving rise to an (integrable) focusing singularity at the edge of the "cones" as seen in Figs. 1 and 2. We must caution that the above is an oversimplification and the true picture is three dimensional, the curve in Fig. 5(b) being replaced by an ω surface. The above concepts can be generalized; for example, the one-dimensional curvature (having a zero at the critical point) is replaced by its two-dimensional analog,

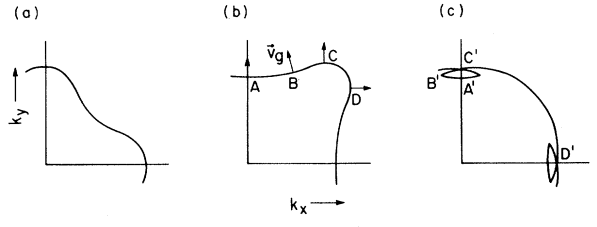

FIG. 3. Schematic two-dimensional representation of (a) phase-velocity surface, (b) constant-ω surface, and (c) group-velocity surface for one of the transverse acoustic modes in a cubic crystal.

the Gaussian curvature K. Focusing singularities will arise whenever $K = 0$ and, in general, may derive from any place on the ω surface.

For quantitative comparison of our experiments with calculations[9] in three dimensions we have employed the computer programs of Taylor, Maris, and Elbaum[3] with certain modifications. Briefly the procedure is as follows: A uniform distribution of points ($0.05° \times 0.05°$ mesh) was assumed in phase space ($\vec{k}$ space); and at each point $\vec{v}_p$ and, in turn, a coordinate on the ω surface were calculated. Next, with $\vec{v}_g$ space subdivided into a fine angular mesh ($0.5° \times 0.5°$) the mapping from the ω surface to $\vec{v}_g$ space was carried out, and the number falling into each $0.5° \times 0.5°$ box was counted, this number being a measure of the phonon amplification for this particular direction. To conserve computation time and to avoid any possibility of multiple counting, we restricted coverage in $\vec{k}$ space to the fundamental sector of $\frac{1}{48}$ of the Brillouin zone; $\vec{v}_g$'s falling outside this sector were mapped back in by appropriate symmetry operations. Results in Fig. 2(a) (solid curve), integrated over detector solid angle, match the data in Fig. 2(b) reasonably well. There are, however, some differences which may arise for the following reasons: First, Fig. 2(a) is derived from only one ω surface whereas 2(b) may contain contribution from both transverse surfaces. Second, all vectors mapping into an appropriate solid angle are counted regardless of their velocity; in other words, there is no time resolution in the calculation as is the case in the experiment. Both problems, in principle, could be remedied, but we have not attempted to do so.

The calculations enable us to identify the structural features in Fig. 2(b). The peaks at $\pm 7°$ and $\pm 5°$ are confirmed as focusing singularities. The peaks at $\pm 3°$, however, arise in a different way: These are contributions picked up by the extensions ($\pm 2.9°$) of the bolometer perpendicular to the $(1\bar{1}0)$ plane of scan. A topographical plot of the focusing enhancement displays sharp elevations or "ridges" in the $(0\bar{1}0)$ and (100) planes. The bolometer "sees" these ridges until its maximum extension ($\pm 2.9°$) is exceeded, whence the peak at $\sim \pm 3°$. It is not a trivial matter to pinpoint on the ω surface the origin of the singularities. One thing one can say is that they do not come from the $(1\bar{1}0)$ plane as one might mistakenly assume from Fig. 3, i.e., the actual shape of the ω surface at point B is a saddle, for which the Gaussian curvature does not vanish.

The structure in Fig. 2(b) is sensitive to the

elastic properties of the crystal. This dependence, we find, is mostly a function of a single parameter, $w = c_{11} - c_{12} - 2c_{44}$ (c_{11}, c_{12}, and c_{44} are the elastic stiffness constants), the magnitude of which represents the departure from elastic isotropy. A good fit[9] obtains for $w = -0.548 \times 10^{12}$ dyne/cm^2; a 2% change worsens the fit noticeably, shifting the peak positions of both singularities by 0.4° (to larger angles with increasing $|w|$). Clearly the structure in the phonon angular distributions is quite sensitive to details in the shape of the ω surface.

To conclude, then, we see that phonons propagate in Ge preferentially as sharply defined beams along the [001] and [110] axes; moreover, these beams contain fine structure in the form of singularities. There are several obvious implications of these results and calculations, some of which we will mention. Firstly, from the pedagogical diagrams of Fig. 3, it is clear that in certain directions (namely, near [001] and [110] axes) one should, with good temporal resolution, see more than three packets of arriving phonons. This is indeed seen in these experiments. Secondly, the implications of Figs. 1 and 2 for thermal conductivity in the ballistic or Knudsen regime hardly require comment. Substantial anisotropies should be observable and will depend on geometrical relationships of the samples relative to the focusing cones. Also Kapitza conductance measurements[1] should be expected to be profoundly influenced by focusing effects and, in particular, to exhibit a definite dependence on surface crystallographic orientation. We might add that we do not regard Ge as a particularly unique, i.e., anisotropic, material and expect (and have observed) similar effects in other dielectrics at low temperatures. Thirdly, with this knowledge of focusing effects it is now possible to understand certain features in the shape of the electron-hole droplet cloud observed in Ge. In particular the strong [001] beams are responsible for the "flares" recorded in the cloud photographs of Greenstein and Wolfe.[10]

We acknowledge with gratitude the many technical contributions of F. C. Unterwald and J. P. Garno. We are indebted to H. J. Maris for providing us with his computer program for phonon focusing.

---

[1]See, for example, *Phonon Scattering in Solids*, edited by L. J. Challis, V. W. Rampton, and A. F. G. Wyatt (Plenum, New York, 1976).

[2]G. F. Miller and M. J. P. Musgrave, Proc. Roy. Soc. London, Ser. A 236, 352 (1956).

[3]B. Taylor, H. J. Maris, and C. Elbaum, Phys. Rev. Lett. 23, 416 (1969), and Phys. Rev. B 3, 1462 (1971).

[4]One example being the acoustic microscopy; V. Jipson and C. F. Quate, Appl. Phys. Lett. 32, 789 (1978).

[5]C. Elbaum, in *Proceedings of the International Conference on Phonon Scattering in Solids, Paris, 1972*, edited by H. J. Albany (Comptes Rendus, Saclay, 1972), p. 1.

[6]V. S. Bagaev, L. V. Keldysh, N. N. Sibeldin, and V. A. Tsvetkov, Zh. Eksp. Teor. Fiz. 70, 702 (1976) [Sov. Phys. JETP 43, 362 (1976)]; L. V. Keldysh, Pis'ma Zh. Eksp. Teor. Fiz. 23, 100 (1976) [JETP Lett. 23, 86 (1976)]; J. Doehler, J. C. V. Mattos, and J. M. Worlock, Phys. Rev. Lett. 38, 726 (1977).

[7]J. C. Hensel and R. C. Dynes, Phys. Rev. Lett. 39, 969 (1977).

[8]The labels FT and ST are purely operational, merely serving to distinguish the two strongest transverse phonon groups by velocity. Identification of a peak with a particular phonon mode is not possible for all θ's.

[9]The calculations employ values of elastic constants and density appropriate for Ge at 2 K: $c_{11} = 1.318 \times 10^{12}$ dyne/cm^2, $c_{12} = 0.496 \times 10^{12}$ dyne/cm^2, $c_{44} = 0.685 \times 10^{12}$ dyne/cm^2, and $\rho = 5.34$. See H. J. McSkimin, J. Appl. Phys. 24, 988 (1953).

[10]M. Greenstein and J. P. Wolfe, Phys. Rev. Lett. 41, 715 (1978).